Personal Submission to the Senate Committee on

Recent Trends in and Preparedness for Extreme Weather Events

Dr Ian R.G. Wilson

South-Eastern Australia needs to prepare for hot dry conditions in the summer of 2019 and possible extensive flooding in 2029

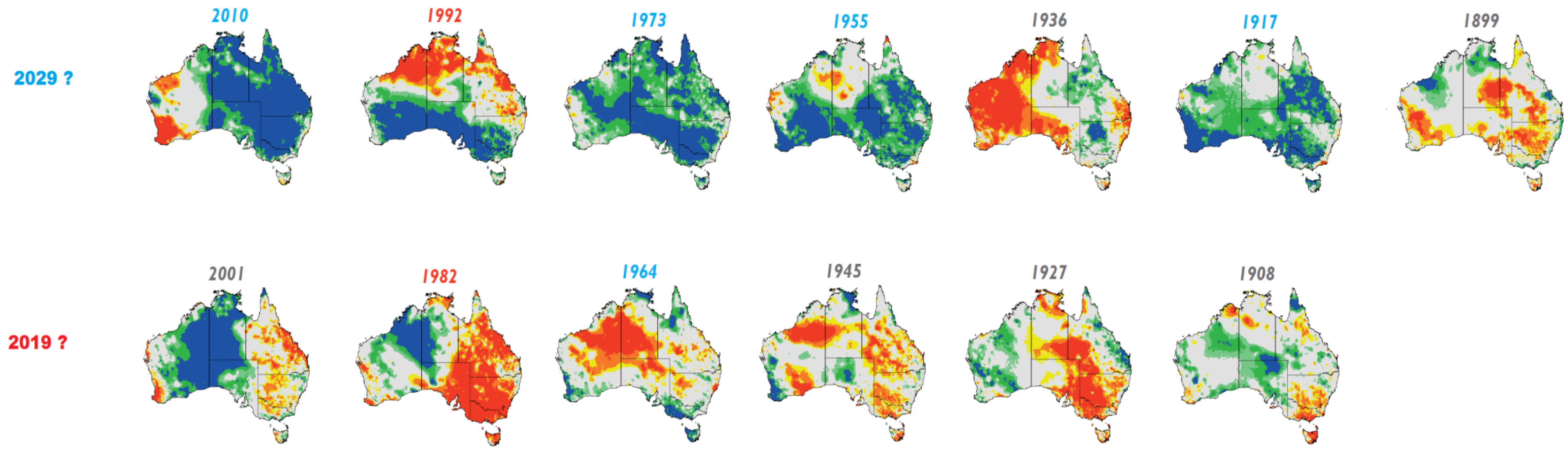

Executive Summary

- The main purpose of this senate submission is to inform the Senate about the discovery of westwardly propagating longitudinal standing waves in the mean sea-level pressure (MSLP) and sea-surface temperature (SST) anomalies of the summer-time (DJF) Southern Ocean that have a zonal wave number N = 4.

- Recent research supports the contention that this propagating N=4 standing wave pattern is being driven by long-term cycles in the lunar atmospheric and oceanic tides.

- Empirical evidence is emerging from this research to show that there is a link between the propagating N=4 standing wave pattern and major flooding events and periods of extreme heat in South East Australia.

- This raises the possibility that we can use our knowledge of future changes in the hemispheric lunar atmospheric and oceanic tides to predict when there might be major flooding events and periods of extreme heat in South East Australia.

- Wilson and Sidorenkov [18] have developed a mutual reinforcing lunar tidal model that predict that the median maximum summer time temperatures in Melbourne and Adelaide should be noticeably above normal during southern summer of 2018/19.

- Flooding data for the Brisbane Valley shows that if the 1825 lunar flood sequence persists we should expect to a significant flooding event in Brisbane and/or Ipswich in 2029 (+/- 1 year).

Response to the terms of reference

(a) *Recent trends on the frequency of extreme weather events, including but not limited to drought, bushfires, heatwaves, floods and storm surges;*

It should go without saying that before anyone can seriously discuss human-induced changes in the frequency of extreme weather events, they must first identify any long-term natural [i.e. not related to human activity] cycles that could influence the frequency of such events.

Unfortunately, the very terms of reference of this Senate Committee implicitly assumes that the frequency of extreme weather events is already being influenced by human activity without ruling out the possibility that the observed changes could mostly be explained by natural climate cycles.

People with some knowledge of factors that affect the extremes in Australia's climate [i.e. on multi-decadal time scales] understand that El Nino/Southern Oscillation (ENSO) plays a critical role in determining the frequency and intensity of floods and droughts in Eastern Australia (BOM_1 [1], Queensland Government [2]).

In addition, they are aware that Indian Ocean Dipole (IOD) also plays an important role in enhancing/ moderating the impact of El Ninos & La Ninas upon the climate extremes in Australia, depending on whether the IOD is in-phase/out-of-phase with the ENSO phenomenon (BOM_2 [3]).

However, not many people seem to be aware of the fact that there is a third climate phenomenon called the Antarctic Circumpolar Wave (ACW - White and Peterson [4], Jacobs and Mitchell [5]) that can have a significant influence upon weather extremes in southern Australia (White [6]).

White and Peterson [4] show that the ACW is made up of a pattern that forms a longitudinal standing wave in the SST and MSLP anomalies of the Southern Ocean that has a zonal wave-number (N) of 2. They find that this pattern propagates around the Earth in an easterly direction roughly once every 8 – 10 years (Cai et al. [7], Weisse et al. [8]).

One example of the significant influence that the ACW has on Australia's climate is given by White [6] who claims that eastward propagating SST anomalies in the ACW can be used to predict more than 50 % of the total inter-annual variance in precipitation over Victoria, NSW, and WA poleward of 20^{O} S latitude, for the 40 year period from 1958 to 1997.

Another example of the influence of the ACW upon the frequency of extreme weather events here in Australia is that given by White et al. [9]. These researchers propose that the Global El Nino Southern Oscillation Wave (GEW) and the ACW mutually reinforce each other, producing a 3 – 5 year global climate cycle that modulates the tropical standing mode of the ENSO in the Pacific Ocean. Hence, in effect they are claiming that the ACW is a critical component of planetary wide natural climate system that plays crucial part in determining the frequency of extreme weather events in Australia.

Further studies of the ACW phenomenon, however, show that the ACW climate system is a little more complex than it first appears. A study by Connolley [10], using climate data from 1958 to 1997, indicates that the ACW phenomenon is only clearly visible between the years 1985 and 1994. They also find that before and after this time period the ACW pattern is quite different from its normal N=2 standing wave pattern with no clear sign of precession.

In addition, Aitken and England [11] use simple linearized transport models to show that the apparent uni-modal nature (i.e. N=2) of the ACW may be an artefact of the short observational record that has been used to infer it. Indeed, Venegas [12] claim that the observed irregular fluctuations of the standing wave mode of the ACW on inter-annual time scales may result from the interference of two distinct standing wave signals, one with a period of around 3.3 years and a zonal wave number of N= 3 with nodes that are centred at fixed locations in the Southern Ocean, and another consisting of a propagating standing wave with a period of ~5 years and a zonal wave number of N = 2.

Hence, the fact that good quality observational data of the Southern oceans have only been available since the early 1980's, has limited our understanding of the true form and nature of the ACW over multi-decadal time scales. However, there have been some recent advances in our understanding of the ACW because of the discovery of lunar atmospheric tides in the upper troposphere.

Li [13], Li and Zong [14], Li et al. [15] have shown that cyclical changes in lunar tidal forcing produce atmospheric tides with periods of 27.3 day and 13.6 days. Li and his associates have detected these atmospheric tides in the tropical troposphere at heights above the 700 hPa isobaric surface (~ 3000m). They also indicate that the tides are likely to be present in the upper parts of the mid-latitude troposphere, as well. Support for the findings of Li et al. [15] is provided by Krahenbuhl et al. [16] who have shown that the 27.3 day lunar atmospheric tides can influence the short-term mid-latitude general circulation pattern by deforming the high-latitude Rossby long-waves. They also find that these tidal effects have their greatest influence in the upper troposphere of both hemispheres.

Wilson [17] has extended the work of Li et al. [15] by showing that the lunar atmospheric tides have an influence upon climate variables in Eastern Australia on inter-annual to decadal time scales. Wilson [17] has shown that variations in the peak latitude anomaly of the summer (DJF) subtropical high pressure ridge over Eastern Australia (LSA) exhibit the same period and phase as that of the 9.3 year lunar draconic spring tides.

In addition, Wilson and Sidorenkov [18] has used the longitudinal shift-and-add method to show that there are N=4 standing wave-like patterns in the summer (DJF) mean sea level pressure (MSLP) and sea-surface temperature (SST) anomaly maps of the Southern Hemisphere between 1947 and 1994. The patterns in the MSLP anomaly maps circumnavigate the Earth in 36, 18, and 9 years. This indicates that these patterns are associated with the long-term lunar atmospheric tides that are either being driven by the 18.0 year Saros cycle or the 18.6 year lunar Draconic cycle. In contrast, the N=4 standing wave-like patterns in the SST anomaly maps circumnavigate the Earth once every 36, 18 and 9 years between 1947 and 1970 but then start circumnavigating the Earth once every 20.6 or 10.3 years between 1971 and 1994. The latter circumnavigation times indicate that they are being driven by the 20.3 year lunar Perigee-Syzygy tidal cycle.

Wilson and Sidorenkov [18] proposed that the different drift rates for the patterns seen in the MSLP and SST anomaly maps between 1971 and 1994 are the result of a reinforcement of the lunar Draconic cycle by the lunar Perigee-Syzygy cycle at the time of Perihelion. They claimed that this reinforcement is part of a 31/62/93/186 year lunar tidal cycle that produces variations on time scales of 9.3 and 93 years.

In order to get a sense of the times when the lunar Perigee-Syzygy cycle and the lunar Draconic Cycle mutually reinforced each other, curves are plotted in figure 1 (below) that indicate the strength of alignment between the two cycles between the years 1857 and 2024. The blue curve in figure 1 shows the angle between the line-of-nodes of the lunar orbit and the Earth-Sun line at the time of Perihelion (θ). The curve is derived in such a way as to highlight the southern summers where there is close alignment. This is done by plotting the function $1/(1+\theta)$. Similarly, the brown curve in figure 1 shows the angle between the line-of-apse of the lunar orbit and the Earth-Sun line at the time of perihelion (φ) plotted as the function $-1/(1+\varphi)$.

The functions represented by the blue and brown curves in figure 1 are used to generate the red curve in this figure. The red curve is an alignment index that is designed to represent the level of reinforcement of the Draconic tidal cycle by the Perigee-Syzygy tidal cycle. This is done by plotting the values of the blue curve at times when there is a close alignment of the line-of-apse and the Earth-Sun line at perihelion (i.e. when $\varphi \leq 16^{O}$). The red curve shows that are two epochs, each lasting about 37-38 years, where there is a strong mutual reinforcement of the Draconic tidal cycle by the Perigee-Syzygy tidal cycle. Individual peaks in the mutual reinforcement occur roughly once every 9.3 years and comparable peaks in the two climate epochs are separated from each other by 93 years.

Hence, if the mutual reinforcement model proposed by Wilson and Sidorenkov [18] is correct, then there should be N=4 standing wave-like features in the Southern Hemisphere's MSLP and SST anomaly maps, similar to those seen in the second climate epoch (i.e. from 1971 to 1994), between about 1878 and 1901.

Unfortunately, the quality of the MSLP and SST data in the late 19th and early 20th centuries is not of a high enough standard to be able to fairly test this prediction. However, there is some circumstantial evidence that when the Draconic tidal cycle is being mutually enhanced by the Perigee-Syzygy tidal cycle there are some observable effects upon the climate variables in the South Eastern part of Australia.

Figure 2 shows the median summer time (December 1st to March 15th) maximum temperature anomaly (The Australian BOM High Quality Data Sets 2010 [19]), averaged for the cities of Melbourne (1857 to 2009 – Melbourne Regional Office – Site Number: 086071) and Adelaide (1879 to 2009 – Adelaide West Terrace – Site Number 023000 combined with Adelaide Kent Town – Site Number 023090), Australia, between 1857 and 2009 (blue curve).

Superimposed on figure 2 is the alignment index curve from figure 1 (red line). A comparison between these two curves reveals that on almost every occasion where there has been a strong alignment between the Draconic and Perigee-Syzygy tidal cycles, there has been a noticeable increase in the median maximum summer-time temperature, averaged for the cities of Melbourne and Adelaide. Hence, if the mutual reinforcing tidal model is correct then this data set would predict that the median maximum summer time temperatures in Melbourne and Adelaide should be noticeably above normal during southern summer of 2018/19.

Figure 1

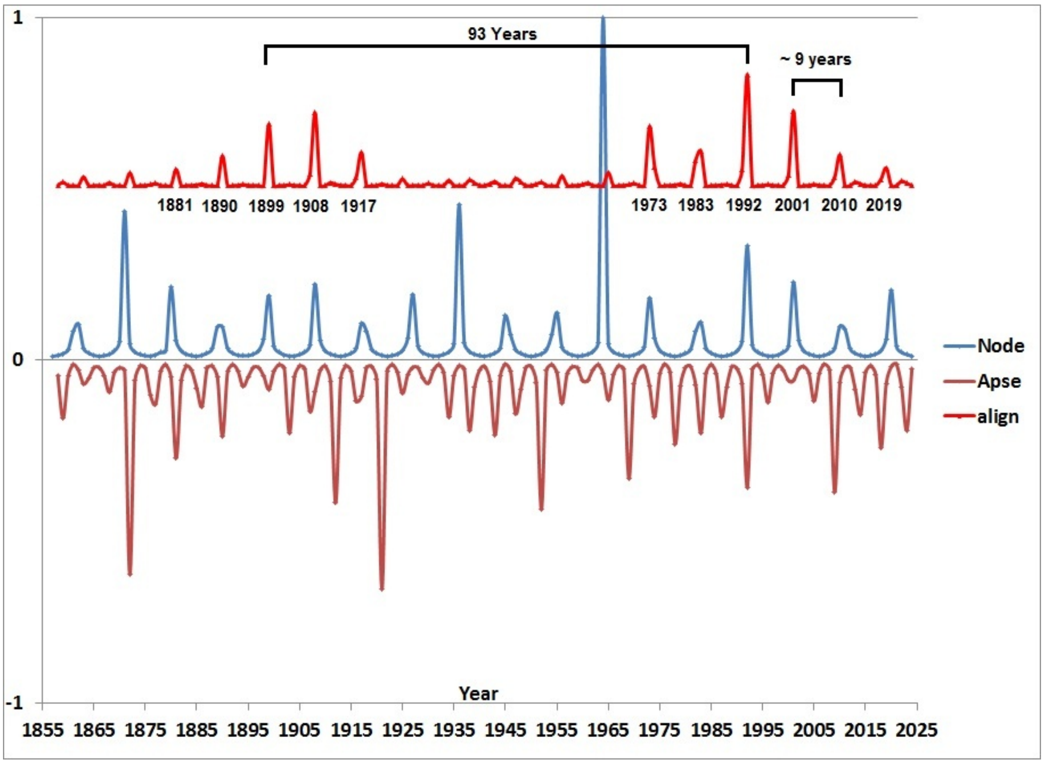

Figure 2

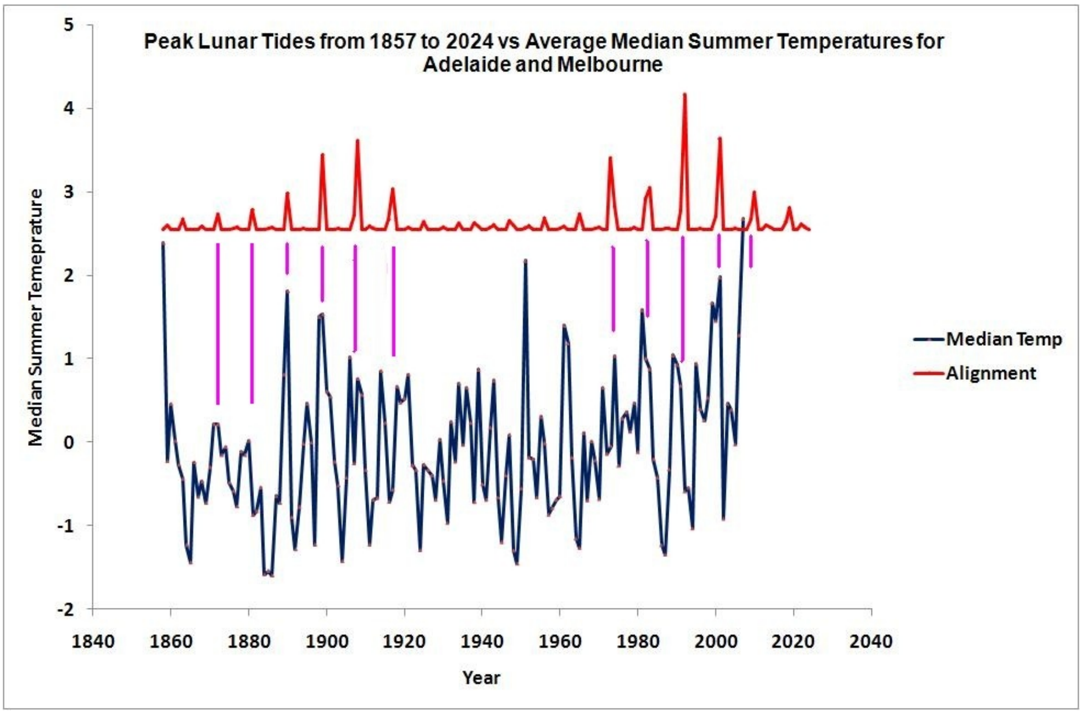

Further evidence that the Moon may have an important role in determining the frequency of extreme weather events in Australia is provided by Table 1. This table shows the dates of major floods in the Brisbane River Valley since the Europeans first discovered the region in 1825. Table 1 reveals that the major floods recorded at Brisbane and/or Ipswich are separated by a period of time that is equal to the Lunar Draconic Cycle of 18.6 years. Unfortunately, the general picture is clouded by the fact that there appear to be three parallel sequences of 18.6 years that fade in and out and sometimes there are floods that occur 3 years prior to expected sequence date.

However, the 1825 lunar flood sequences is the only one that persists over the 188 year record with the other sequences starting in 1856 and 1889 fading out after only a few cycles. If the 1825 lunar flood sequence continues, we should expect to a significant flooding event in either Brisbane or Ipswich in 2029 (+/- 1 year).

Finally, the top of the figure on the front of this submission show a sequence of maps of Australia's annual rainfall, starting in 2010.5 and going back till 1899 in steps of time that are equivalent to the 18.6 year lunar Draconic cycle. In all but one case (i.e. 1899) the rainfall over south-eastern Australia was significantly above average in these years. If this sequence persists then we should expect greater than normal rain over south-eastern Australia in 2029.

Underneath the first sequence of maps on the cover of this submission is another sequence of maps showing Australia's annual rainfall, starting in 2001.0 and going back till 1908 in steps of time that are equivalent to the 18.6 year lunar Draconic cycle. The latter sequence is shifted by 9.3 years (= 18.6/2 years) from the former sequence. If this sequence persists then we should expect lower than normal rain (and possibly hot dry conditions over south-eastern Australia in summer of 2019 (Queensland Government [2]).

The dates of major floods at Brisbane and/or Ipswich

a) 1825 Sequence

18.6 Year Draconic Lunar Cycle	Predicted Date of Flood	Actual date of Flood
1825	1825	1825*
	1843.6 – 3 years =	1841
1825 + (1 x 18.6) =	1843.6	1844
1825 + (2 x 18.6) =	1862.2	1863
1825 + (4 x 18.6) =	1899.4	1898
1825 + (7 x 18.6) =	1955.2	1955
	1973.8 – 3 years	1971
1825 + (8 x 18.6) =	1973.8	1974
1825 + (9 x 18.6) =	1992.4	1991?
1825 + (10 x 18.6) =	2011.0	2011
1825 + (10 x 18.6) =	**2029.6**	**2029?**

b) 1856 Sequence

1856.2	1856.2	1857
	1893.4 – 3 years	1889 & 1890
1856.2 + (2 x 18.6) =	1893.4	1893
	1930.6 – 3 years	1927
1856.2 + (4 x 18.6) =	1930.6	1931

c) 1889 Sequence

1889.9	1889.8	1889 & 1890
1889.8 + (1 x 18.6) =	1908.4	1908
1889.8 + (2 x 18.6) =	1927.0	1927

References:

1. BOM_1: http://www.bom.gov.au/climate/enso/, last accessed 18/01/2013

2. Queensland Government: http://www.longpaddock.qld.gov.au/products/pdf/australiasvariablerainfall_jan-dec.pdf, last accessed 18/01/2013

3. BOM_2: http://www.bom.gov.au/climate/enso/history/ln-2010-12/IOD-what.shtml, last accessed 18/01/2013

4. White W.B. and Peterson R.G., 1996, *An Antarctic circumpolar wave in surface pressure, wind, temperature and sea-ice extent*, Nature, 380, 699 – 702.

5. Jacobs, G. A., and J. L. Mitchell, 1996, Ocean circulation variations associated with the Antarctic Circumpolar Wave. *Geophys. Res. Lett.,* 23**,** 2947–2950.

6. White W. B., 2000, *Influence of the Antarctic Circumpolar Wave on Australian Precipitation from 1958 to 199,* J. of Clim., 13, 2125 – 2141.

7. Cai W., Baines P. G. and Gordon H. B., 1999, *Southern Mid- to High-Latitude Variability, a Zonal Wavenumber-3 Pattern, and the Antarctic Circumpolar Wave in the CSIRO Coupled Model*, J. of Clim., 12, 3087 – 3104.

8. Weisse R., Mikolajewicz U., Sterl A. and Drijfhout S. S., 1999, *Stochastically forced variability in the Antarctic Circumpolar Current*, J. Geophys. Res., 104, 11049 – 11064.

9. White, W. B., Chen S., Allan R. J., and Stone R. C. 2002, *Positive feedbacks between the Antarctic Circumpolar Wave and the global El Niño-Southern Oscillation Wave*, J. Geophys. Res., *107*(C10), 3165 – 3177.

10. Connolly W.M., 2003, *Long-term variation of the Antarctic Circumpolar Wave,* J. Geophys. Res., 107.

11. Aitken C. M. and England M. H., 2005, *On the Stochastic Forcing of Modes of Interannual Southern Ocean Sea Surface Temperature Variability*, J. of Clim., 18, 3074 – 3083.

12. Venegas S. A., 2003, *The Antarctic Circumpolar Wave: A Combination of Two Signals?*, J. of Clim., 16, 2509 – 2525.

13. Li G., 2005, *27.3-day and 13.6-day atmospheric tide and lunar forcing on atmospheric circulation*. Adv. Atmos. Sci, 22**(**3), 359-374.

14. 14. Li G., and Zong H., 2007, *27.3-day and 13.6-day atmospheric tide*. Science in China (D), 50(9), 1380-95.

15. Li G., Zong H, and Zhang Q., 2011, *27.3-day and average 13.6-day periodic oscillations in the earth's rotation rate and atmospheric pressure fields due to celestial gravitation forcing*. Adv. Atmos. Sci., 28(1), 45-58.

16. Krahenbuhl D. S., Pace M. B., Cerveny R. S., and Balling Jr. R.C., 2011, *Monthly lunar declination extremes' influence on tropospheric circulation patterns*. J. of Geophys. Res., 116, D23121 – D23126.

17. Wilson, I.R.G., 2012, *Lunar tides and the long-term variation of the peak latitude anomaly of the summer Sub-Tropical High Pressure Ridge over Eastern Australia.* 2012, The Open Atmospheric Science Journal, 6, 49-60.

18. Wilson, I. R. G. and Sidorenkov N. S., 2013, *Long-Term Lunar Atmospheric Tides in the Southern Hemisphere*, The Open Atmospheric Science Journal, submitted.

19. The Australian BOM High Quality Temperature Data Sets available at ftp://ftp.bom.gov.au/anon/home/ncc/www/change/HQdailyT. Last accessed April 2010.